Measurement and modeling of high-linearity modified uni-traveling carrier photodiode with highly-doped absorber

Huapu Pan*, Zhi Li, Andreas Beling, and Joe C. Campbell

Department of Electrical and Computer Engineering, University of Virginia, 351 McCormick Road, Charlottesville, VA 22904, USA
**hp5n@virginia.edu*

Abstract: The third-order intermodulation distortions of InGaAs/InP modified uni-traveling carrier photodiodes with a highly-doped p-type absorber are characterized. The third-order local intercept point is 55 dBm at low frequency (< 3 GHz) and remains as high as 47.5 dBm up to 20 GHz. The frequency characteristics of the OIP3 are well explained by an equivalent circuit model.

OCIS codes: (040.5160) Photodetectors.

References and links

1. K. J. Williams, L. T. Nichols, and R. D. Esman, "Photodetector Nonlinearity on a High-Dynamic Range 3 GHz Fiber Optic Link," J. Lightwave Technol. **16**(2), 192–199 (1998).
2. K. J. Williams, D. A. Tulchinsky, and A. Hastings, "High-power and high-linearity photodiodes", *21st Annual Meeting of the IEEE Lasers and Electro-Optics Society*, (Institute of Electrical and Electronics Engineers, Newport Beach, California, 2008), pp.290–291.
3. K. Williams, R. Esman, and M. Dagenais, "Nonlinearities in p-i-n microwave photodetectors," J. Lightwave Technol. **14**(1), 84–96 (1996).
4. A. Joshi, S. Datta, and D. Becker, "GRIN Lens Coupled Top-Illuminated Highly Linear InGaAs Photodiodes," IEEE Photon. Technol. Lett. **20**(17), 1500–1502 (2008).
5. H. Jiang, D. S. Shin, G. L. Li, T. A. Vang, D. C. Scott, and P. K. L. Yu, "The Frequency Behavior of the Third-Order Intercept Point in a Waveguide photodiode," IEEE Photon. Technol. Lett. **12**(5), 540–542 (2000).
6. M. Chtioui, A. Enard, D. Carpentier, S. Bernard, B. Rousseau, F. Lelarge, F. Pommereau, and M. Achouche, "High-Power High-Linearity Uni-Traveling-Carrier photodiodes for Analog Photonic Links," IEEE Photon. Technol. Lett. **20**(3), 202–204 (2008).
7. T. Ohno, H. Fukano, Y. Muramoto, T. Ishibashi, T. Yoshimatsu, and Y. Doi, "Measurement of intermodulation distortion in a unitravelingcarrier refracting-facet photodiode and a p–i–n refracting-facet photodiode," IEEE Photon. Technol. Lett. **14**(3), 375–377 (2002).
8. A. Beling, H. Pan, C. Hao, and J. C. Campbell, "Measurement and modeling of a high-linearity modified uni-traveling carrier photodiode," IEEE Photon. Technol. Lett. **20**(14), 1219–1221 (2008).
9. A. Beling, H. Pan, H. Chen, and J. C. Campbell, "Measurement and modelling of high-linearity partially depleted absorber photodiode," Electron. Lett. **44**(24), 1419–1420 (2008).
10. H. Pan, A. Beling, H. Chen, J. C. Campbell, and P. D. Yoder, "The Influence of Nonlinear Capacitance on the Linearity of a Modified Uni-Traveling Carrier Photodiode," *2008 International Topical Meeting on Microwave Photonics*, (Institute of Electrical and Electronics Engineers, Gold Coast, Australia, 2008), pp. 82–85.
11. Z. Griffith, Y. M. Kim; M. Dahlstrom, A.C. Gossard, M. J. W. Rodwell, "InGaAs-InP metamorphic DHBTs grown on GaAs with lattice-matched device performance and fτ, fmax>268 GHz," IEEE Electron Device Lett. **25**, 675–677 (2004).
12. H. Pan, A. Beling, H. Chen, and J. C. Campbell, "Characterization and Optimization of High-Power InGaAs/InP Photodiodes," Opt. Quantum Electron. **40**(1), 41–46 (2008).
13. M. N. Draa, J. Ren, D. C. Scott, W. S. Chang, and P. K. Yu, "Three laser two-tone setup for measurement of photodiode intercept points," Opt. Express **16**(16), 12108–12113 (2008).
14. A. Ramaswamy, J. Klamkin, N. Nunoya, L. A. Johansson, L. A. Coldren, and J. E. Bowers, "Three-tone characterization of high-linearity waveguide uni-traveling-carrier photodiodes," *21st Annual Meeting of the IEEE Lasers and Electro-Optics Society*, (Institute of Electrical and Electronics Engineers, Newport Beach, California, 2008), pp. 286–7.

#116405 - $15.00 USD Received 28 Aug 2009; revised 18 Oct 2009; accepted 19 Oct 2009; published 21 Oct 2009

15. M. Dentan, and B. de Cremoux, "Numerical Simulation of the Nonlinear Response of a p-i-n photodiode Under High Illumination," J. Lightwave Technol. **8**(8), 1137–1144 (1990).
16. T. H. Stievater, and K. J. Williams, "Thermally induced nonlinearities in high-speed p-i-n photodetectors," IEEE Photonics Technol. Lett. **16**(1), 239–241 (2004).
17. H. Pan, A. Beling, H. Chen, and J. C. Campbell, "The Frequency Behavior of the Intermodulation Distortions of Modified Uni-Traveling Carrier Photodiodes Based on Modulated Voltage Measurements," IEEE J. Quantum Electron. **45**(3), 273–277 (2009).

1. Introduction

High-performance analog optical links with large spurious-free dynamic range require high-power, high-linearity photodiodes [1]. At low frequencies, photodiodes with good linearity characteristics have been reported. By measuring the third-order harmonics, a partially depleted absorber (PDA) photodiode has been shown to have a third-order harmonic output intercept point (HOIP3) of 51 dBm at 3 GHz [2], which is equivalent to a third-order local intercept point (OIP3) of 46.2 dBm according to the cubic dependence of the third-order nonlinearity terms [3]. Similarly, an HOIP3 of 54 dBm at 829 MHz, which corresponds to an OIP3 of 49.2 dBm, was reported for a dual depletion region photodiode [4]. However, although high OIP3 values have been demonstrated, in general the OIP3 degrades as a function of increasing frequency [5]. A conventional uni-traveling carrier (UTC) photodiode achieved OIP3 of 36 dBm at 20 GHz [6]; Ohno et al. reported an OIP3 of 40.5 dBm at 5.8 GHz for a UTC refracting-facet photodiode [7]; and Beling et al. obtained 36 dBm at 20 GHz using a charge-compensated modified uni-traveling carrier (CC-MUTC) photodiode [8]. In a recent publication, an InGaAs/InP partially depleted absorber photodiode with a highly-doped absorber (HD-PDA) was reported to have an OIP3 of 39 dBm at 20 GHz [9]. In this paper, we report an InGaAs/InP MUTC photodiode with a highly doped p-type absorber, which will be referred to in the following as an HD-MUTC photodiode. The OIP3 of this device exhibits only a slight roll off with frequency and remains as high as 47.5 dBm up to 20 GHz. The frequency dependence of the OIP3 of the HD-MUTC photodiode is compared with that of CC-MUTC photodiodes. The frequency characteristics of both types of detectors are well explained by an equivalent circuit model based on the measured relative voltage-dependent responsivity and capacitance of the photodiodes [8].

2. Device design and three-tone measurement

The vertical layer structure of the HD-MUTC photodiode is shown in Fig. 1. The epitaxial layers were grown on a semi-insulating InP substrate by molecular beam epitaxy. The InGaAs absorbing region with a thickness of 950 nm is comprised of a 650 nm p^+ absorbing region and a 300 nm unintentionally-doped absorber layer. Previously p-type InGaAs absorbing layers doped with Zn exhibited strong diffusion of the Zn dopant, which results in a non-abrupt junction doping profile. This non-abrupt doping profile causes the junction capacitance of the photodiode to have a strong dependence on bias voltage, which has been shown to be responsible for the decrease of OIP3 with frequency [10]. In order to form an abrupt junction doping profile, in this work C was used instead of Zn as the dopant in the 650 nm p^+ absorbing layer. The p-type doping level was graded in 10 steps from $8\cdot10^{19}$ to $5\cdot10^{18}$ cm^{-3} so as to assist electron transport in the doped absorber. A 24 nm-thick InGaAs/InAlAs chirped superlattice and a 5 nm moderately n-type doped InP cliff layer were incorporated between the InGaAs and InP to reduce carrier pile up at the heterojunction interface. The 24 nm-thick InGaAs/InAlAs chirped superlattice is used to smooth the bandgap discontinuity between the InGaAs layer and the InP layer [11], while the 5 nm moderately n-type doped InP cliff layer is used to enhance the electric field in the intrinsic InGaAs layer to help electrons inject into the intrinsic InP layer and reduce the space charge effect in the intrinsic InGaAs layer [12]. The background doping level in the unintentionally-doped absorbing layer was below $5\cdot10^{15}$ cm^{-3}. Back-illuminated mesa structures were fabricated by inductive coupled plasma reactive ion

#116405 - $15.00 USD Received 28 Aug 2009; revised 18 Oct 2009; accepted 19 Oct 2009; published 21 Oct 2009

etching. Microwave contact pads and an air-bridge connection to the top p-contact layer were fabricated for high-speed measurements. Finally a 220 nm SiO_2 anti-reflection layer was deposited on the back of the wafer. The devices were mounted on an Al heat sink for testing. Photodiodes with an active diameter of 40 μm exhibited a 3 dB bandwidth of 13 GHz at −6 V and responsivity of 0.49 A/W at 1550 nm. Compared with the CC-MUTC photodiode reported in Ref. [8], which has similar InGaAs absorber, the responsivity of the HD-MUTC is not as high. This is due to the fact that the p-type InGaAs absorber is so highly doped that the electron lifetime in the p-type InGaAs absorber of the HD-MUTC is much shorter than that of the CC-MUTC and thus a larger fraction of the photo-generated electrons before they diffuse into the intrinsic InGaAs layer.

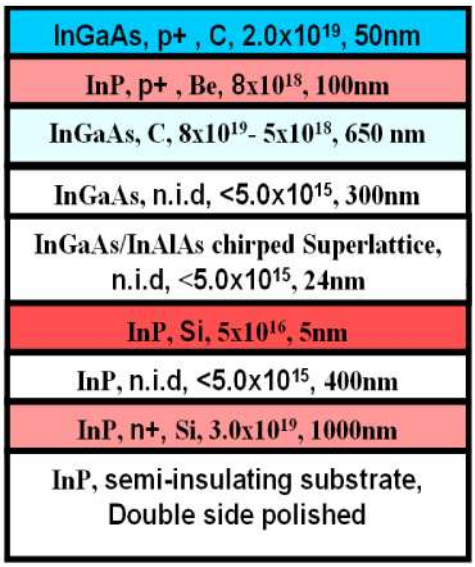

Fig. 1. Schematic cross section of InGaAs–InP HD-MUTC photodiode.

When considering nonlinearities in photodiodes, the two-tone third-order intermodulation distortions (IMD3) are particularly interesting, since their frequencies may be close to the fundamental modulation frequencies. For conventional two-tone measurements, the output RF power P_f at the fundamental frequencies f_1, f_2 and the power of IMD3, P_{IMD3}, at $(2*f_2-f_1)$ and $(2*f_1-f_2)$ were measured; following the approach in Ref [1]. the conventional two-tone OIP3 is defined as OIP3= P_f+ $(P_f- P_{IMD3})/2$ dBm. However, it has recently been suggested that the harmonics from the optical modulators may result in inaccuracies in the two-tone measurement results [13]. Hence, a three-tone setup, which is less sensitive to nonlinearities in the modulator response [14], was also utilized to provide more accurate measurements. For the three-tone measurement, the output RF power P_f at the fundamental frequencies f_1, f_2, f_3 and P_{IMD3} at $(f_1+f_2-f_3)$, $(f_2+f_3-f_1)$, $(f_3+f_1-f_2)$ were measured. The three-tone IMD3 is 6dB larger than the ideally measured two-tone IMD3. This difference in IMD3 can be understood from the fact that the coefficient of $\cos(\omega_i t+\omega_j t-\omega_k t)$ (i,j,k=1,2,3 i≠j≠k) is 2 times as large as that of $\cos(2\omega_i t-\omega_j t)$ (i,j=1,2,3 i≠j) after expanding the expression $[\cos(\omega_i t)+\cos(\omega_j t)+\cos(\omega_k t)]^3$ (i,j,k=1,2,3 i≠j≠k). If the three-tone OIP3 is defined analogously to the two-tone OIP3, then, following the approach in Ref. [7], a factor of 3dB should be added to the measured three-tone OIP3 in order to compare with the two-tone measurements. The measured data were calibrated taking the losses of the components in the RF path into account.

#116405 - $15.00 USD Received 28 Aug 2009; revised 18 Oct 2009; accepted 19 Oct 2009; published 21 Oct 2009

3. Non-linear phenomena and equivalent circuit analysis

When operating a reverse-biased photodiode under optical illumination the photocurrent induces a voltage drop at the series and load resistances [15]. As a consequence, the bias voltage across the photodiode junction is reduced and modulated at the signal frequency which may cause variations in the device capacitance and responsivity. It has previously been shown that the relative voltage-dependent responsivity, R(V), is the limiting nonlinear factor for the OIP3 for this type of photodiode at low frequencies (<3GHz), while the voltage dependent capacitance, C(V), is the primary limiting nonlinear factor at higher frequencies [8]. In order to improve the linearity for both frequency ranges, the HD-MUTC photodiode described in the previous section with a 650 nm highly-doped p-type absorber and a 300 nm undoped absorber was designed to reduce variation of capacitance with voltage.

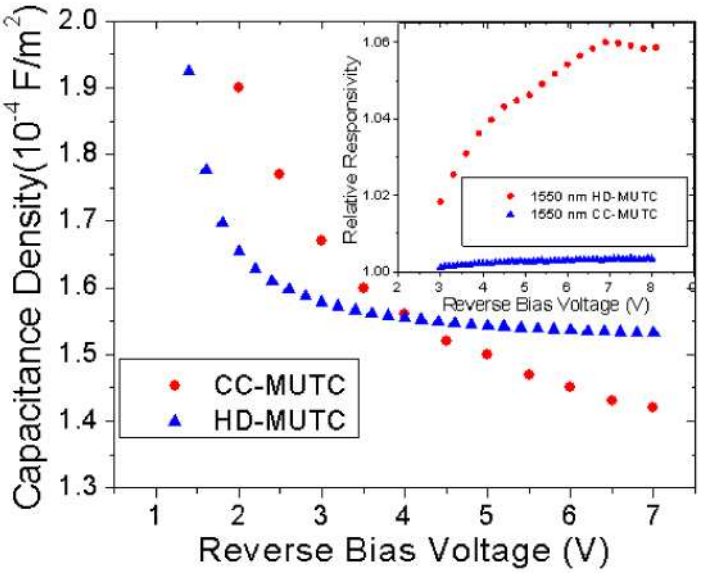

Fig. 2. Measured photodiode capacitance density for CC-MUTC and HD-MUTC photodiodes. Inset: Relative responsivity for CC-MUTC and HD-MUTC photodiodes.

Figure 2 compares the voltage-dependent capacitance and responsivity of the HD-MUTC and the CC-MUTC photodiodes reported in Ref [10]. The measured C(V) is normalized to capacitance density, which is independent of the size of the photodiodes. In contrast to CC-MUTC photodiodes, which exhibit significant variation of the capacitance density up to 7V, that of the HD-MUTC is only weakly dependent on the reverse bias when it is > 4V. This is a result of the high doping level of the undepleted absorber. The dependence of the responsivity of the HD-MUTC, however, shows a stronger dependence on voltage (an increase of ~6% as the bias increases to 8V) than that of the CC-MUTC photodiodes (~0.5% increase). This is due to the fact that impact ionization and the Franz Keldysh effect are more significant in the depleted InGaAs layers and the depleted InGaAs layer in the HD-MUTC (300 nm) is thicker than that of the CC-MUTC (designed to be 150 nm but actually much less due to Zn diffusion) [10].

The voltage dependent responsivity of the photodiodes was measured at very low photocurrent levels (< 200 μA) to avoid slow ohmic heating [16]. However, the shape of the R(V) curve may change at high photocurrent levels due to the concomitant increase in temperature, since both impact ionization and the Franz-Keldysh effect vary with temperature. The OIP3 of the HD-MUTC was measured versus photocurrent at 320 MHz and reverse biases of 5 V, 7 V and 10 V. The results are shown in Fig. 3. There is a strong dependence of

#116405 - $15.00 USD Received 28 Aug 2009; revised 18 Oct 2009; accepted 19 Oct 2009; published 21 Oct 2009

OIP3 on photocurrent for all reverse bias values; the OIP3 reaches peaks at approximately 21 mA, 30 mA and 33 mA at 5 V, 7 V and 10 V reverse bias, respectively. Using bias modulation techniques [17], it can be shown that the strong dependence of the OIP3 on photocurrent is caused by the change of the shape of R(V) with photocurrent. At certain photocurrents the responsivity becomes a linear function of reverse bias and thus except for the second-order intermodulations all the higher order intermodulations produced by R(V) are significantly reduced. This is an important subject for a future study. At 33 mA of photocurrent and 10 V reverse bias, the drive power of the optical modulator was varied to measure the dependence of P_{IMD3} on P_f. As shown in the inset of Fig. 3, the slopes of P_f and P_{IMD3} are 1 and 3, respectively, and the OIP3 intercept is 55 dBm.

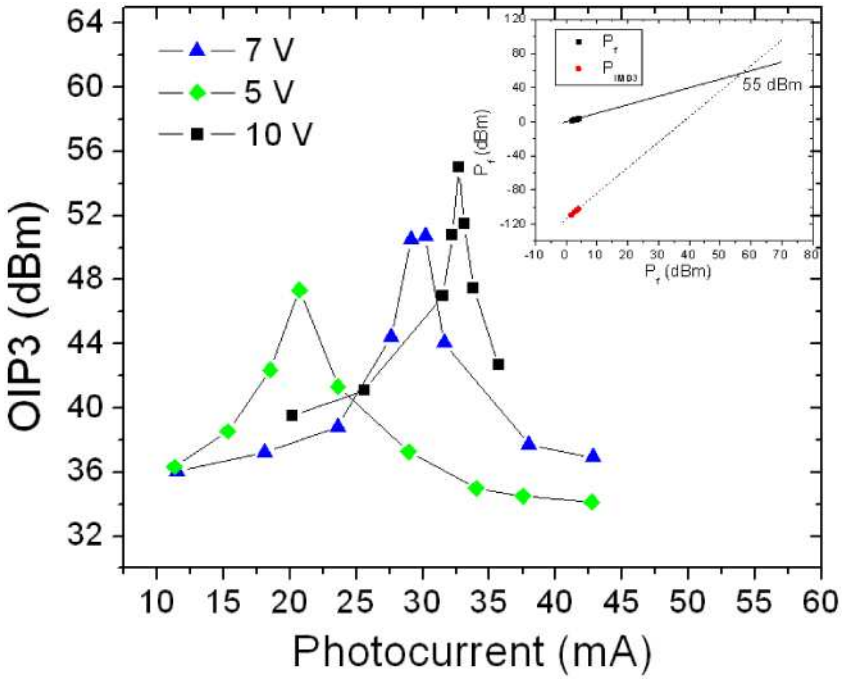

Fig. 3. OIP3 of the HD-MUTC photodiode versus photocurrent at 5 V, 7 V and 10 V reverse bias. Inset: at 33 mA and 10 V, the power of IMD3 versus fundamental power showing a good slope of 3 and an extracted OIP3 of 55 dBm

Figure 4 compares the frequency dependence of the measured OIP3 for the HD-MUTC with that of the CC-MUTC photodiodes. Since the OIP3 of both the CC-MUTC and the HD-MUTC exhibit dependence on photocurrent and bias, the measurements were done at the photocurrent and bias conditions that maximized the OIP3 of each photodiode in order to make the "fairest" comparison (50 mA and 7 V for the CC-MUTC and 34 mA and 10 V for the HD-MUTC). For the HD-MUTC the voltage dependence of capacitance on reverse bias, dC/dV, is much smaller than that of the CC-MUTC when the reverse bias is > 4 V. However, as shown in Fig. 2, dC/dV decreases as the reverse bias increases. Thus the HD-MUTC photodiode was biased at a high reverse bias of 10 V to further reduce dC/dV so as to achieve higher OIP3 at high frequencies. As shown in Fig. 4, although the OIP3 of the CC-MUTC is high at low frequency, it rolls off as much as 16 dB as the frequency increases from 300 MHz to 21 GHz. This is due to the voltage-dependent capacitance, C(V), as explained in Ref [8]. The calculated OIP3 of the CC-MUTC photodiode based only on its C(V) curve, using the same equivalent circuit model reported in Ref [8], is shown as the dashed line in Fig. 4, which agrees well with the measurements for frequencies > 6 GHz. However, the OIP3 of the HD-

#116405 - $15.00 USD Received 28 Aug 2009; revised 18 Oct 2009; accepted 19 Oct 2009; published 21 Oct 2009

MUTC starts at 55 dBm at low frequencies and decreases only 7.5 dB up to 20 GHz as a result of the weakly voltage-dependent capacitance. At 20 GHz, the OIP3 of the HD-MUTC remained as high as 47.5 dBm. The calculated OIP3 of the HD-MUTC based on its C(V) curve at 10 V is shown as the solid line in Fig. 4. The calculated C(V)-limited OIP3 begins to approach the measured values only when the frequency is greater than 6 GHz, and the measured OIP3 is almost independent of frequency when the frequency is less than 6 GHz. This indicates that the OIP3 of the HD-MUTC is primarily limited by R(V) in the frequency range up to 6 GHz and C(V) becomes significant only at higher frequencies. The drop of OIP3 accelerates as the frequency increases while the calculated OIP3 limited by C(V) shows the opposite trend at high frequencies. This is an indication that in addition to C(V), other frequency-dependent nonlinear mechanisms such as carrier speed modulation caused by the voltage swing may also contribute to the decrease of OIP3 in these photodiodes at high frequencies [3].

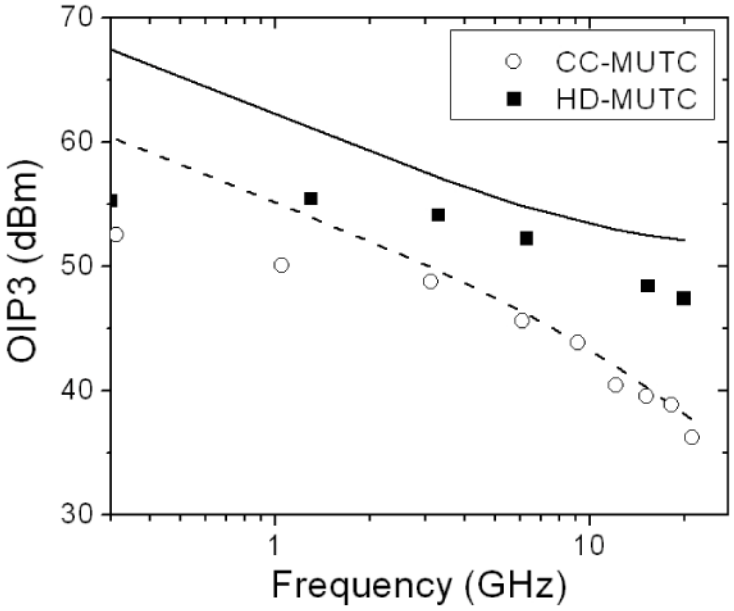

Fig. 4. OIP3 of CC-MUTC photodiode at 50 mA of photocurrent and 7 V reverse bias, and HD-MUTC at 34 mA of photocurrent and 10 V reverse bias. Dashed line: calculated OIP3 of CC-MUTC photodiode based on C(V); Dotted line: calculated OIP3 of HD-MUTC based on C(V).

4. Conclusions

In conclusion, the third-order intermodulation distortions of HD-MUTC photodiodes have been characterized using three-tone setup and compared to those of CC-MUTC photodiodes. The OIP3 of the HD-MUTC photodiode reaches 55 dBm at low frequencies with only slight roll off with frequency; at 20 GHz the OIP3 reaches 47.5 dBm. The excellent frequency behavior is due to the high doping levels in the undepleted absorber and the abrupt doping profile due to C doping. The frequency dependence of OIP3 is well explained by an equivalent circuit model.

#116405 - $15.00 USD Received 28 Aug 2009; revised 18 Oct 2009; accepted 19 Oct 2009; published 21 Oct 2009